

SENSITIVITIES OF ALPHA CONTINUOUS AIR MONITORS FOR DETECTION OF AIRBORNE ^{239}Pu

C. V. McIsaac, P. D. Randolph, C. R. Amaro,
D. N. Thompson, and R. J. Pawelko
Idaho National Engineering Laboratory, P.O. Box 1625,
Idaho Falls, Idaho, 83415

ABSTRACT

This paper presents the results of measurements of the sensitivities of several state-of-the-art alpha continuous air monitors (CAMs) for airborne ^{239}Pu . Three commercially available alpha CAMs and a prototype alpha CAM that is currently in use at Argonne National Laboratory-West (ANL-W) were evaluated at the Idaho National Engineering Laboratory (INEL). The alpha CAMs were tested using ambient air, air synthetically laden with aerosolized nonradioactive dust, and air synthetically laden with dust spiked with 9 nCi/g ^{239}Pu . Alpha spectra collected using the CAMs were analyzed using three analysis algorithms that are widely used today. Measured airborne ^{239}Pu concentrations and ^{239}Pu lower limit of detection concentrations determined for each CAM using the three different analysis algorithms are presented.

INTRODUCTION

The Department of Energy (DOE) Order DOE 5480.11(1) establishes maximum permissible concentrations (MPCs), or derived air concentrations (DACs), for airborne TRU isotopes to protect a worker from undue risk from airborne radioactive contaminants. An alpha CAM allows real-time monitoring of airborne TRU concentrations.

All alpha CAMs detect the presence of airborne alpha contamination by pulse height analysis of the alpha activity removed from air that is sampled. A typical measurement of the concentrations of airborne alpha-emitting radionuclides is performed by pulling a continuous sample of ambient air through a filter having a pore size small enough to trap aerosolized particles. The filter is positioned close to an alpha detector, which is normally a solid-state silicon detector, to maximize counting efficiency and minimize the loss of alpha particle energy during transit from the filter to the detector. The alpha-emitting radionuclides are attached to the aerosol particles that are trapped by the filter. The amount of aerosol material collected on the filter depends on its concentration in the ambient air and on the sampling flow rate.

This measurement approach presents three major interactive problems. The first is that the filter collects the dust normally present in the ambient environment. Alpha particles emitted by aerosols imbedded in the dust lose energy in passing through the dust layer and consequently contribute a continuum of counts to the spectrum, resulting in higher backgrounds and broader, less well defined peaks. The second difficulty stems from the fact that the collection filter is normally fixed so that the current concentration of an alpha-emitting radionuclide must be calculated based on a change in detector count rate. The instrument must determine a differential value of the count rate to determine concentration. The third, and perhaps the most fundamental problem, is the presence of naturally occurring alpha-emitting isotopes in the environment. Alpha particles

emitted by radon progeny contribute a continuum of counts to the spectrum in the energy region of the ^{239}Pu alpha particles.

Both mechanistic and analytical approaches have been developed to handle natural background alpha radiation. Mechanistic methods of reducing natural background alpha radiation generally rely on the use of inertial impactors. Two of the four CAMs that were evaluated - the Kurz series 8311 and the ANL-W prototype CAM - were equipped with impactors. Several analytical methods have also been developed that allow subtracting the background counts from the ^{239}Pu energy window. Three different spectrum analysis techniques that are currently installed in the majority of commercially available alpha CAMs were evaluated.

DESCRIPTION OF ALPHA CAMS

As was previously mentioned, of the four alpha CAMs tested in the study, three were commercial units while the fourth was a prototype that is currently in use at ANL-W facilities. The commercial CAMs that were tested were the Kurz series 8311, RADeCO model 452, and the Victoreen model 758. A preliminary evaluation of the performance of the Victoreen model 758 CAM was performed during 1989.(2) The ANL-W CAM has been in use at ANL-W since 1975.(3) The three commercial CAMs were chosen for testing because they represent state-of-art designs. The ANL-W CAM was also selected for testing because it has been reported(4) to have a sensitivity of less than 0.5 DAC-h for ^{239}Pu in the presence of 1 pCi/L of ^{218}Po (RaA). This section provides a brief description of the main components of the four alpha CAMs.

The ANL-W CAM employs a two-stage virtual impactor to concentrate airborne Pu-bearing particulates. Air, which is sampled at 10 CFM, is drawn through a circular array of inlet jets and is directed towards a complementary array of receiving tubes. A major portion of the air leaving the jets is drawn off laterally before the air stream enters the receiving tubes. Small particles entering the inlet jets follow the lateral flow of air and do not enter the receiving tubes.

Large particles are not able to follow the lateral air flow and enter the receiving tubes. This arrangement is repeated in a second stage in the impactor. In principle, the minor air flow exiting the final receiving tubes, which is only 0.7 CFM, contains most of the plutonium-bearing particulates that entered the impactor. This minor air flow is directed to a sample collection filter whose influent face is spaced about 3 mm from a solid state silicon detector. The cut point, or size at which 50% of the particles pass through the impactor, corresponds to an aerodynamic diameter of about $1.5 \mu\text{m}$, which is equivalent to a geometric diameter of $0.4 \mu\text{m}$ for a plutonium oxide particle.(4) Thus, particles larger than $0.4 \mu\text{m}$ are collected on the sample filter with greater than 50% efficiency. Detailed descriptions of other components of the ANL-W CAM are presented in Ref. (5).

The Kurz series 8311 alpha detector is manufactured by Kurz Instruments Incorporated, Monterey, CA. The CAM employs an inertial dichotomous impactor that directs entrained particulates onto the face of a diffused junction solid-state silicon detector. Air enters the CAM through a circumferential inlet slot whose width is ordinarily set to eliminate particles larger than $20 \mu\text{m}$ from the inlet air stream.(6) The air then passes through the inertial impactor, which is a plate containing two sets of concentrically arranged holes. The effluent face of the impactor plate is positioned directly over the alpha detector. In principle, larger particles strike and adhere to the face of the alpha detector while the smaller-diameter particulates remain entrained in the air stream and are exhausted from the CAM. The cut point of the model 8311 impactor has been reported to be about $0.7 \mu\text{m}$ aerodynamic diameter.(6) Because this CAM does not use a collection filter, alpha particles do not have to traverse an air gap before striking the detector, and hence, its alpha spectra exhibit a resolution much better than can be achieved using conventional designs that employ filters. A detector amplifier/line driver circuit allows remote operation of the CAM sample collection head at distances up to 1219m. A mass flow sensor and associated electronics that monitor sampling flow rate and cumulative air sample volume are incorporated into the model 8311FE and 8311FT Kurz CAMs.

The Victoreen model 758 and RADeCO model 452 alpha CAMs are typical of conventional alpha CAM designs that do not employ impactors. The Victoreen model 758 CAM is manufactured by Victoreen, Inc., Cleveland, Ohio, and the RADeCO model 452 selective alpha monitor is manufactured by SAIC/RADeCO, San Diego, CA. Both the Victoreen and RADeCO CAMs draw air through a filter that is in close proximity to a solid-state silicon detector. The recommended sampling flow rate for both units is 2 CFM. In the case of the RADeCO model 452 CAM, a multi-vaned collimator is installed over the face of the detector to reduce the maximum path length that alpha particles emitted from the collection filter traverse before

hitting the detector. The collimator improves the resolution of alpha peaks in the collected spectra at the cost of reducing the absolute counting efficiency of the alpha detector. Two different collection filters were used with the RADeCO CAM. The manufacturer supplies Millipore SM $5.0 \mu\text{m}$ filters with the model 452 CAM, however, Millipore AA $0.8 \mu\text{m}$ were also used during this study. A detailed description of the Victoreen model 758 CAM is presented in Ref. 2.

SAMPLINGS PERFORMED AT THE INEL

Measurements of ambient air were performed in an unconfined space inside a laboratory, while measurements of aerosolized dust were made inside a glove box equipped with a dust aerosolizer. During each measurement of ambient air, two of the four CAMs were operated simultaneously. The aerosolizer used in the experiments consisted of a V-shaped plexiglass tray measuring about 30 cm high by 46 cm long. The inside width of the cavity in the tray tapered from about 20 cm at the top to 0 cm at the bottom. A perforated 0.95 cm diameter plastic tube was installed near the bottom inside surface of the tray and the tube was plumbed to a plant air supply. Measurements of air laden with nonradioactive dust were performed using soil collected from the vicinity of the Radioactive Waste Management Complex (RWMC) that was sieved to 200 mesh. Measurements of air laden with radioactive dust were performed using the same soil spiked with 9 nCi/g ^{239}Pu that was sieved to 100 mesh. During samplings of aerosolized dust, the flow rate through the aerosolizer was usually maintained between 2 and 10 L per minute. During each measurement of aerosolized blank or spiked dust, the Kurz, RADeCO, and Victoreen alpha CAMs were operated simultaneously.

DESCRIPTION OF METHODS USED TO ANALYZE ALPHA SPECTRA

Several analytical methods have been developed that allow subtracting the background counts from the ^{239}Pu energy region. The average energy of the ^{239}Pu alpha particles is 5.15 MeV. Three different spectrum analysis techniques that are currently installed in the majority of commercially available alpha CAMs were evaluated. These algorithms use either two, three, or four regions of interest (ROIs) and net counts in the ^{239}Pu ROI are determined by subtracting some fraction of the counts in adjacent background ROIs. In each case, the expression for net ^{239}Pu counts is a linear function of counts in the ^{239}Pu ROI and the background ROI(s). The following three equations were used to determine net counts in the ^{239}Pu ROI:

Two-window algorithm:

$$C_{Pu} = C_1 - k_1 C_2 \quad (\text{Eq. 1})$$

Three-window algorithm:

$$C_{Pu} = C_4 - k_2 (C_3 + C_5) \quad (\text{Eq. 2})$$

Four-window algorithm:

$$C_{Pu} = C_6 - k_3 \frac{C_7 C_8}{C_9} \quad (\text{Eq. 3})$$

where C_1 , C_4 , and C_6 are the total number of counts in the ^{239}Pu ROI and C_2 , C_3 , C_5 , C_7 , C_8 , and C_9 are the total number of counts in the corresponding background ROIs. Average values of the coefficients k_1 , k_2 , and k_3 were determined from analyses of spectra collected during samplings of ambient air and/or air laden with nonradioactive dust. ROIs centered at 6.00, 7.69, and 8.78 MeV were used to integrate counts in the ^{218}Po (RaA), ^{214}Po (RaC'), and ^{212}Po (ThC') alpha peaks. Gross count rates in these latter ROIs were monitored to determine how effective the ANL-W and Kurz impactors were in reducing the quantities of radon and thoron daughters that were collected. A more detailed discussion of the methods used to analyze alpha spectra is given in Ref. 7.

Cumulative spectra were stored at either 30 or 60 minute intervals during samplings of ambient room air and aerosolized blank dust. The spectra were analyzed to determine the value and standard deviation of each coefficient used in the two-, three-, and four-window analysis algorithms. Using the measured average values of the coefficients, spectra obtained using each CAM were then analyzed using all three algorithms to determine if a given algorithm worked best for a given CAM. For each spectrum, background and net counts in the ^{239}Pu ROI and their associated uncertainties were determined. Lower limits of detection (LLDs) for ^{239}Pu were then calculated at the 95% confidence level by applying the methods of Currie (8) to these results. These LLDs were then compared with the sensitivity requirement of 8 DAC-h which is specified in DOE Order 5480.11.

AIRBORNE ^{239}Pu CONCENTRATIONS DETERMINED BY ANALYZING ALPHA SPECTRA USING TWO-, THREE-, AND FOUR-WINDOW ANALYSIS ALGORITHMS.

Concentrations of airborne ^{239}Pu during samplings of ambient and synthetically generated dust-laden air were determined by analyzing collected alpha spectra using the two-, three-, and four-window analysis algorithms previously described. Average measured values of the coefficients k_1 , k_2 , k_3 , which are given in Table I, were used in the corresponding analysis algorithms to calculate airborne ^{239}Pu concentrations. Because the ANL-W CAM was not available during the samplings of laboratory-generated at-

mospheres, only ANL-W spectra collected during samplings of ambient air were analyzed. In the case of the ANL-W CAM, concentrations of ^{239}Pu in ambient air were calculated using successive cumulative spectra collected at one hour intervals. The concentrations of airborne ^{239}Pu determined by analyzing ANL-W CAM spectra collected during a sampling of ambient air are plotted as a function of sampling time in Fig. 1. The data presented in Fig. 1 show that, as expected, calculated ^{239}Pu concentrations fluctuated around a value close to zero. During the first five hours of operation, fluctuations in calculated concentrations were relatively large compared to variations at later times. As one would expect, as the number of counts in the ROIs increased, their associated uncertainties decreased resulting in less dispersion in the calculated ^{239}Pu concentrations. During the second day of sampling, concentrations ranged between about $\pm 3 \times 10^{-6}$ pCi/L, and during the fifth day the range decreased to about $\pm 8 \times 10^{-7}$ pCi/L.

Background concentrations of ^{239}Pu were also calculated for a sampling of clean dust performed using the Kurz, RADeCO, and Victoreen CAMs. The calculated ^{239}Pu concentrations for the Kurz, RADeCO, and the Victoreen CAMs are plotted in Figs. 2, 3, and 4, respectively. The concentrations plotted in Figs. 2, 3, and 4 were calculated using successive cumulative spectra collected 30 minutes apart during 22 hours of sampling. Common to the results for all three CAMs are relatively large positive and/or negative concentrations during the first few hours of sampling. The initial relatively large dispersion that is evident in Fig. 2 is likely due to poor counting statistics. The initial relatively large negative concentrations evident in Figs. 3 and 4 reflect the fact that background counts in the ^{239}Pu ROI were being oversubtracted during the first several hours of sampling, indicating that the coefficients k_1 , k_2 , k_3 used in the analysis algorithms were too large during this time frame. As the dust loadings on the RADeCO and Victoreen filters increased, calculated ^{239}Pu concentrations became less negative. Based on dust loadings following the completion of sampling, at 7 hours the dust loadings on the RADeCO and Victoreen sample collection filters were 0.24 and 0.28 mg/cm², respectively. Beyond about 7 hours, calculated ^{239}Pu concentrations stabilized at values between about 1×10^{-4} and 7×10^{-4} pCi/L for both CAMs.

Concentrations of airborne ^{239}Pu measured using the Kurz, RADeCO, and Victoreen CAMs during a sampling of air laden with dust spiked with 9 nCi/g ^{239}Pu are plotted as a function of sampling time in Fig. 5, 6, and 7, respectively. In these figures, concentration is expressed in units of pCi/L and sampling time is expressed in units of hours. The ^{239}Pu concentrations plotted in Figs. 5, 6, and 7 were calculated using successive spectra collected at 30 minute intervals. Similar results for the other five samplings of aerosolized dust spiked with ^{239}Pu were also determined by analyzing

TABLE I
Measured Values of Coefficients Used in Analysis Algorithms for Samplings of Ambient Air

Start Date	Sample Volume (L)	Average Dust Concentration (mg/L)	k_1	k_2	k_3
<u>ANL-W:</u>					
12/12/89	7.08 E(+5)	2.8 \pm 0.2 E(-6)	0.3241 \pm 0.0027	0.5127 \pm 0.0059	0.2131 \pm 0.0027
12/15/89	1.69 E(+6)	5.3 \pm 0.6 E(-7)	0.2824 \pm 0.0025	0.4801 \pm 0.0034	0.1985 \pm 0.0017
12/20/89	2.39 E(+6)	1.13 \pm 0.07E(-6)	0.3032 \pm 0.0018	0.4858 \pm 0.0024	0.2100 \pm 0.0014
12/27/89	2.06 E(+6)	1.89 \pm 0.1 E(-6)	0.3684 \pm 0.0033	0.5550 \pm 0.0032	0.2296 \pm 0.0020
01/02/90	1.99 E(+6)	2.46 \pm 0.1 E(-6)	0.3716 \pm 0.0030	0.5658 \pm 0.0040	0.2583 \pm 0.0027
Combined:			0.3279 \pm 0.0020	0.5170 \pm 0.0022	0.2203 \pm 0.0012
<u>Kurz model 8311:</u>					
12/15/89	3.38 E(+5)	(a)	0.0368 \pm 0.0077	0.3531 \pm 0.0049	0.0842 \pm 0.0014
12/27/89	4.22 E(+5)	(a)	0.0677 \pm 0.0025	0.4398 \pm 0.0074	0.1546 \pm 0.0047
01/02/90	4.06 E(+5)	(a)	0.0507 \pm 0.0022	0.4653 \pm 0.0114	0.1060 \pm 0.0044
05/17/90	2.44 E(+5)	(a)	0.0431 \pm 0.0016	0.3903 \pm 0.0084	0.0933 \pm 0.0028
06/15/90	2.38 E(+5)	(a)	0.0460 \pm 0.0014	0.4762 \pm 0.0101	0.0993 \pm 0.0038
<u>RADeCO model 452:</u>					
06/12/90	1.58 E(+5)	(b)	0.3542 \pm 0.0036	0.6775 \pm 0.0045	0.1666 \pm 0.0026
06/15/90	2.45 E(+5)	(b)	0.4155 \pm 0.0017	0.7277 \pm 0.0023	0.1822 \pm 0.0028
Combined:			0.3814 \pm 0.0033	0.6996 \pm 0.0034	0.1735 \pm 0.0020
<u>Victoreen model 758:</u>					
12/12/89	1.13 E(+5)	1.5 \pm 0.1 E(-5)	0.3905 \pm 0.0044	0.6801 \pm 0.0039	0.2495 \pm 0.0015
12/20/89	3.71 E(+5)	6.7 \pm 0.4 E(-6)	0.3605 \pm 0.0019	0.6675 \pm 0.0020	0.2740 \pm 0.0010
05/17/90	1.83 E(+5)	(a)	0.4656 \pm 0.0052	0.7200 \pm 0.0036	0.3686 \pm 0.0035
06/15/90	1.82 E(+5)	(a)	0.5202 \pm 0.0016	0.7333 \pm 0.0022	0.3401 \pm 0.0029

a. Not measured.

b. Results for the RAdECo 5.0 μ m filter were inconclusive, probably because the adhesive used in the filter holder card dried out during sampling.

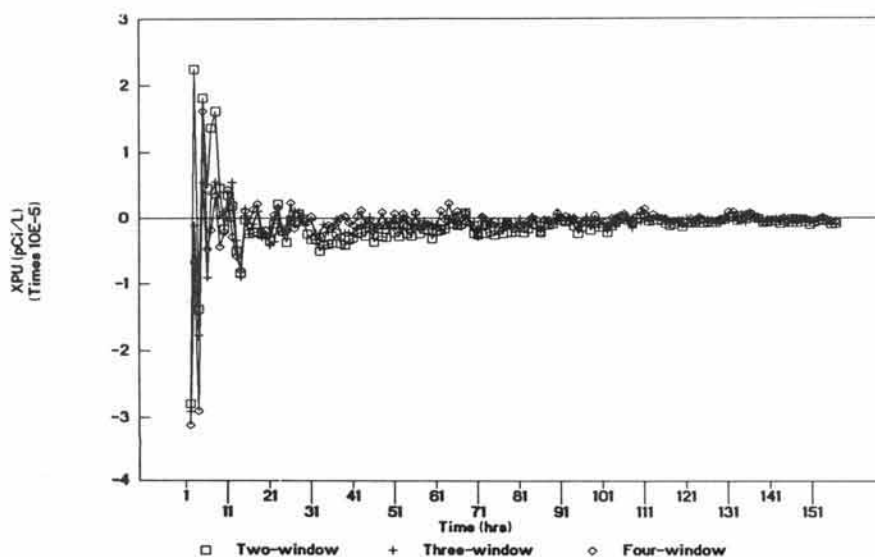


Fig. 1. ^{239}Pu concentration versus sampling time for a sampling of ambient air performed December 20-27, 1989 using the ANL-W CAM.

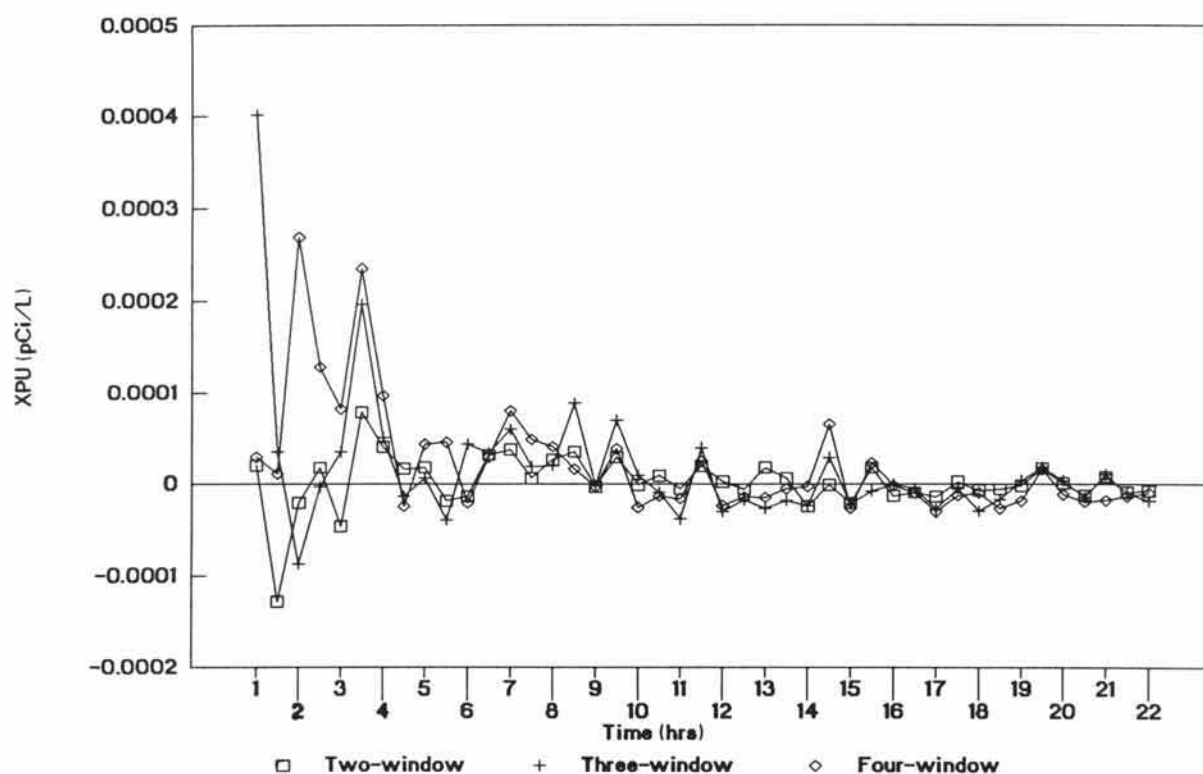


Fig. 2. ^{239}Pu concentration versus sampling time for a sampling of aerosolized clean dust performed June 19-20, 1990 using the Kurz CAM.

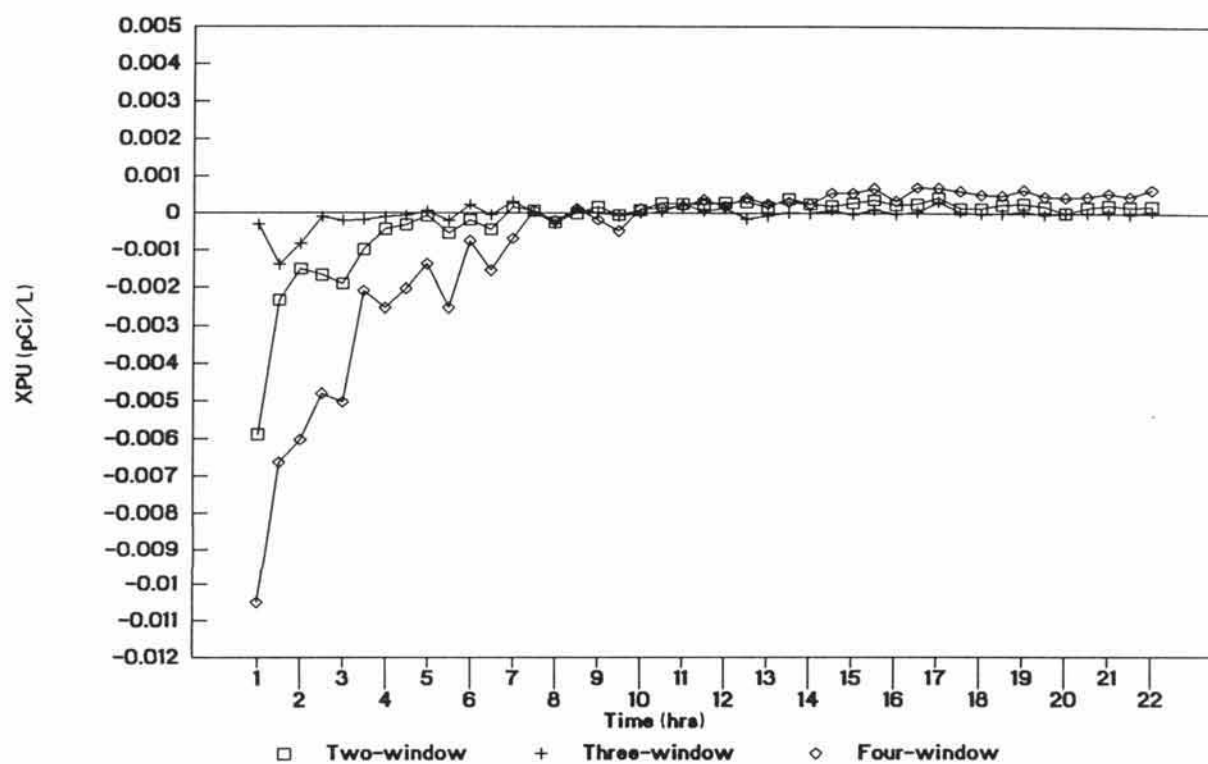


Fig. 3. ^{239}Pu concentration versus sampling time for a sampling of aerosolized clean dust performed June 19-20, 1990 using the RAdCO CAM.

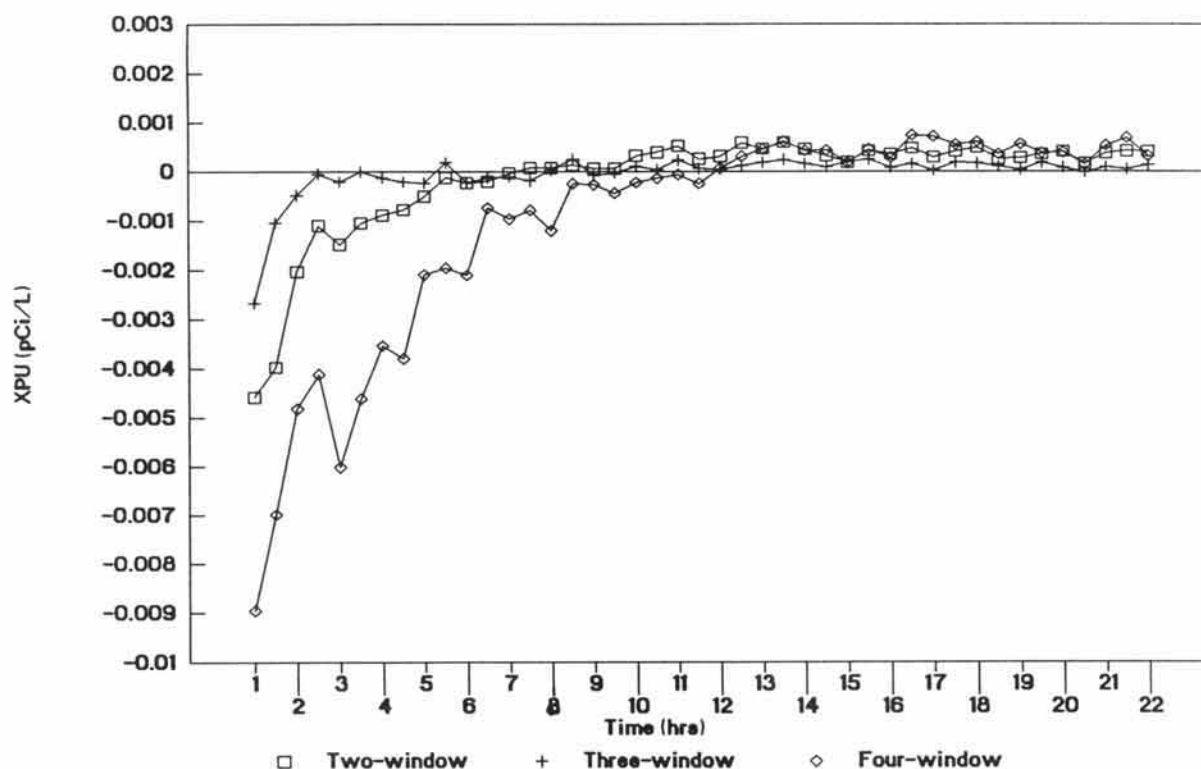


Fig. 4. ^{239}Pu concentration versus sampling times for a sampling of aerosolized clean dust performed June 19-20, 1990 using the Victoreen CAM.

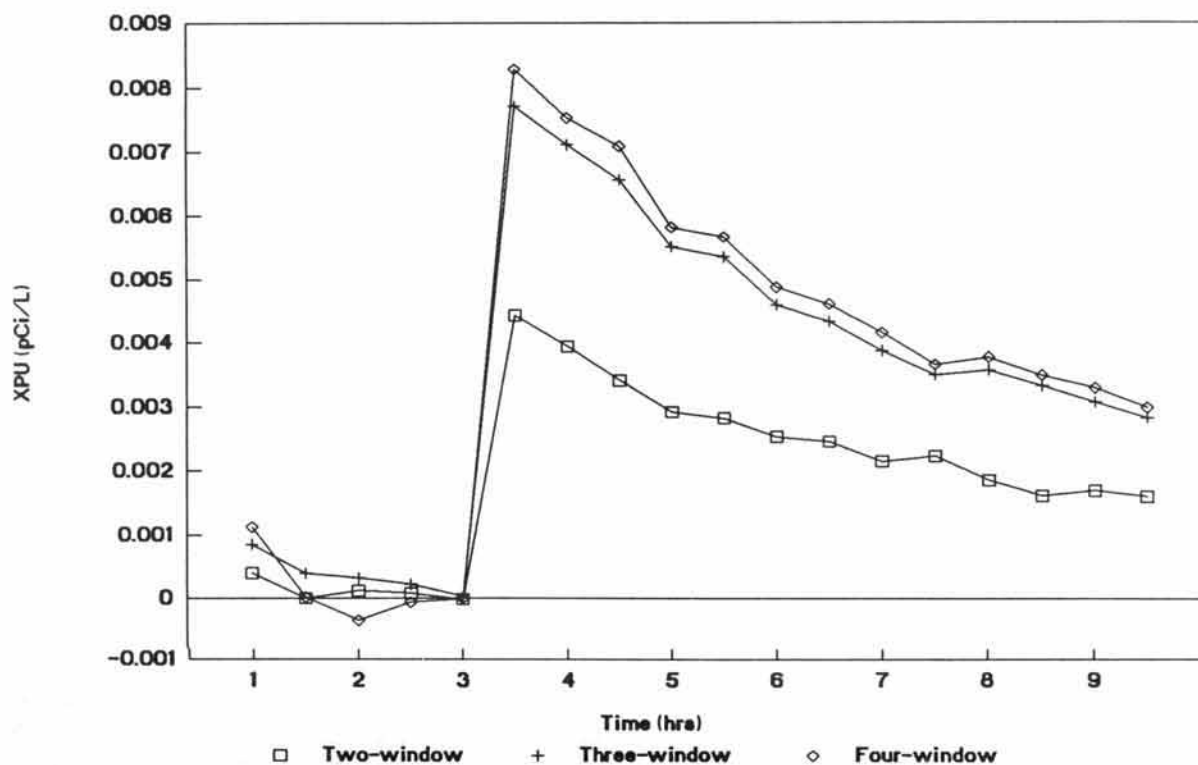


Fig. 5. ^{239}Pu concentration versus sampling time for a sampling of aerosolized dust, that was spiked with 8 nCi/g ^{239}Pu , performed June 27, 1990 using the Kurz.

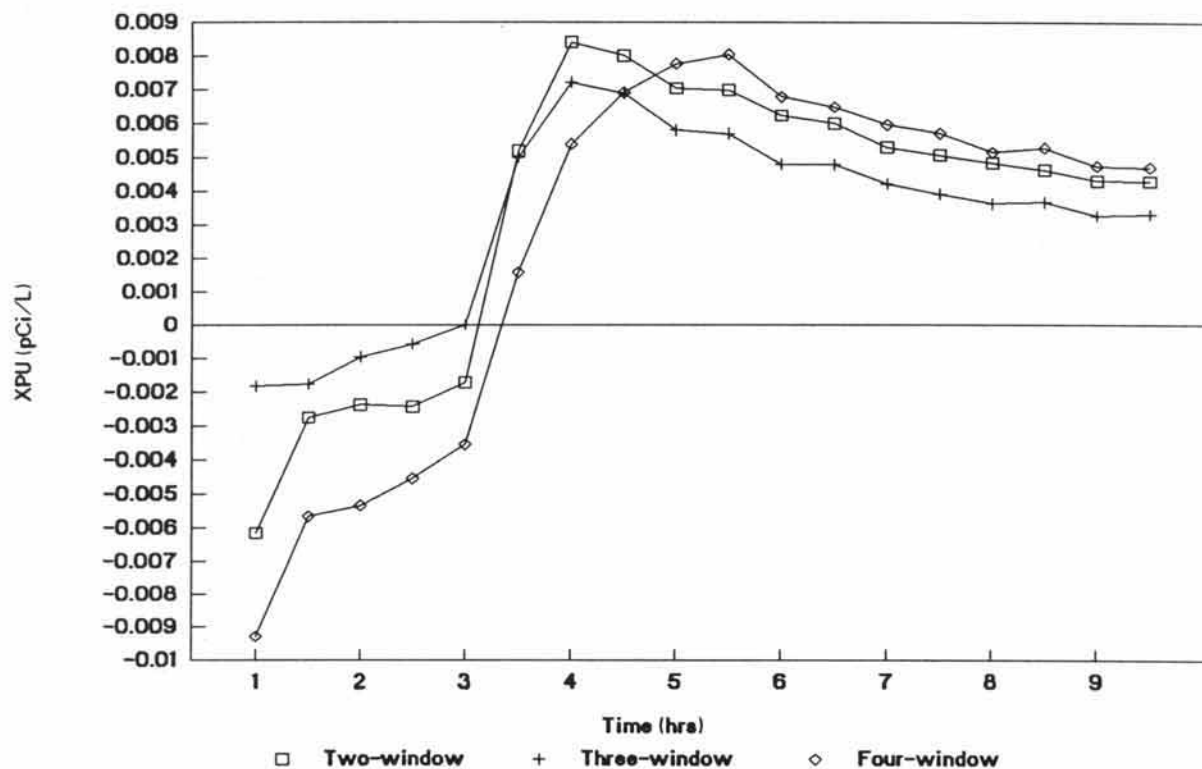


Fig. 6. ^{239}Pu concentration versus sampling time for a sampling of aerosolized dust, that was spiked with 8 nCi/g ^{239}Pu , performed June 27, 1990 using the RAdCO CAM.

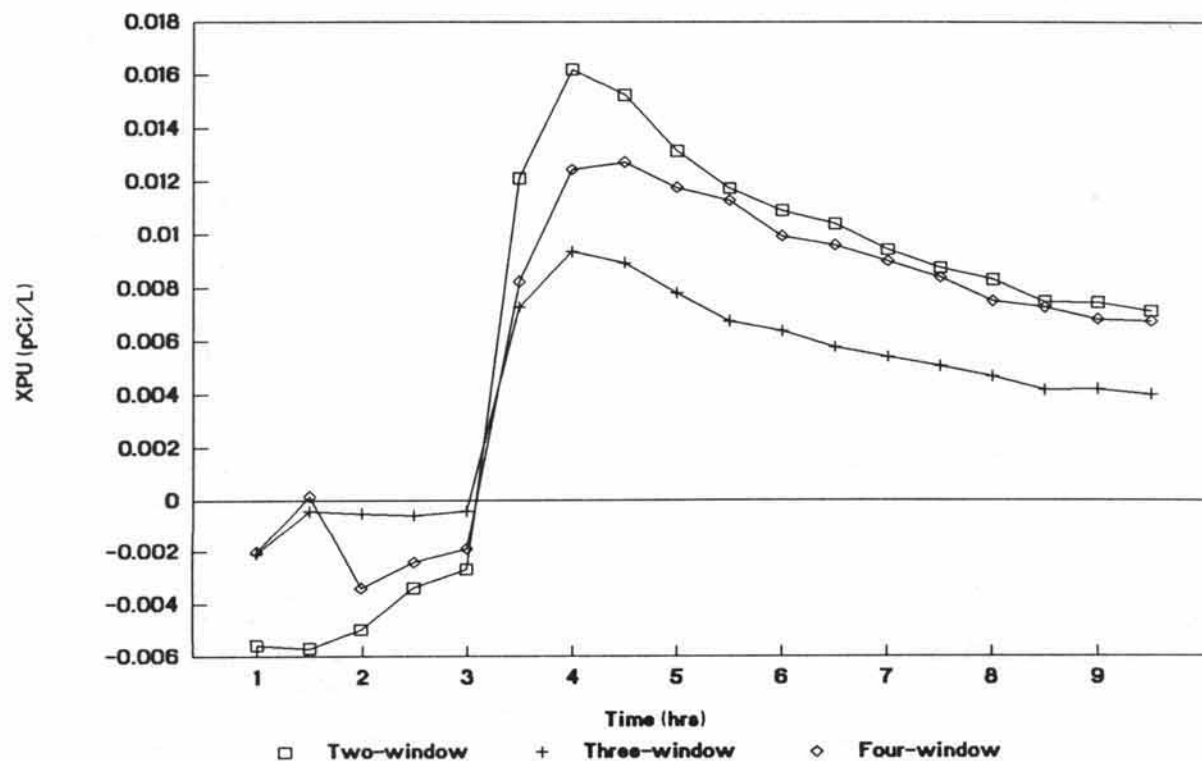


Fig. 7. ^{239}Pu concentration versus sampling time for a sampling of aerosolized dust, that was spiked with 8 nCi/g ^{239}Pu , performed June 27, 1990 using the Victoreen CAM.

collected spectra using the two-, three-, and four-window analysis algorithms. Those results are presented in Ref 7.

For the sampling whose results are shown in Figs. 5, 6, and 7, the aerosolizer remained covered during the first 3 hours and 20 minutes of the sampling and, therefore, the three CAMs sampled only ambient air during this time. The plots shown in Figs. 5, 6, and 7 all show abrupt increases in ^{239}Pu concentration between 3 and 3 1/2 hours, which corresponds to the time when the aerosolizer was uncovered. In the case of the Kurz CAM, ^{239}Pu concentrations calculated using the three different algorithms all peaked at 3 1/2 hours, whereas concentrations measured using the RADeCO and Victoreen CAMs peaked between the 4 and 5 1/2 hours depending on the analysis algorithm used. For all three CAMs and algorithms, measured concentrations of ^{239}Pu then gradually decreased throughout the remainder of the sampling, indicating that the soil in the vicinities of the air holes in the aerosolizer tube gradually became depleted of smaller diameter particles. Based on radiochemical analyses of the Kurz, RADeCO, and Victoreen sample and effluent air stream filters, during the sampling, average concentrations of airborne ^{239}Pu at the locations of the three CAMs were, respectively, $(4.5 \pm 0.2) \times 10^{-3}$, $(6.5 \pm 0.4) \times 10^{-3}$, and $(1.18 \pm 0.06) \times 10^{-2}$ pCi/L. In the case of the Kurz CAM, the average values of the ^{239}Pu concentrations determined using the two-, three-, and four-window analysis algorithms were, respectively, $(2.6 \pm 0.9) \times 10^{-3}$, $(5.2) \times 10^{-3}$, and $(5 \pm 2) \times 10^{-3}$ pCi/L. The latter two values are in good agreement with the average concentration determined by radiochemical analysis, while concentrations calculated using the two-window algorithm appear to be biased low by about a factor of two. Average ^{239}Pu concentrations measured using the RADeCO CAM were $(6 \pm 1) \times 10^{-3}$, $(5.1) \times 10^{-3}$, and $(6 \pm 1) \times 10^{-3}$ pCi/L using the two-, three-, and four-window analysis algorithms, respectively. Similar results for the Victoreen CAM were $(1.1 \pm 0.3) \times 10^{-2}$, $(6 \pm 2) \times 10^{-3}$, and $(9 \pm 2) \times 10^{-3}$ pCi/L, respectively, using the two-, three-, and four-window analysis algorithms. In the case of the Victoreen CAM, concentrations calculated using the three-window algorithm appear to be biased low by about a factor of two.

In general, airborne ^{239}Pu concentrations measured using the Kurz, RADeCO and Victoreen CAMs agreed very well with the concentrations estimated using the results of radiochemical analyses of sample and effluent air stream filters. Average concentration of airborne ^{239}Pu during the six samplings that were performed ranged from 3.7×10^{-3} pCi/L (0.2 DAC) to 2.1×10^{-2} pCi/L (10.5 DAC). The apparent low bias of the concentrations determined analyzing Kurz CAM spectra using the two-window analysis algorithm (see Fig. 5) is also evident in the results for the Kurz CAM for the other five samplings. However, the concentrations determined analyzing spectra collected with the RADeCO and Victoreen CAMs using the two-window

analysis algorithm showed no obvious bias. For the RADeCO CAM, all three analysis algorithms yielded very similar ^{239}Pu concentrations. In the case of the Victoreen CAM, with the exception of the results for one sampling, all three analysis algorithms also yielded very similar ^{239}Pu concentrations.

After the ^{239}Pu -spiked dust began to be aerosolized, statistical uncertainties in the net number of counts in the ^{239}Pu ROI typically ranged between 2% and 5% at the one-sigma level. However, the ^{239}Pu concentrations shown in Figs. 5, 6, and 7 that were measured at one-half hour intervals using the Kurz, RADeCO, and Victoreen CAMs were generally below each CAM's lower limit of detection (LLD) at the 95% confidence Fig. 8 level. The ^{239}Pu LLD concentrations for the three previously mentioned CAMs as well as for the ANL-W CAM were calculated at the 95% confidence level for each of the three analysis algorithms using the methods of Curie.(8) The results are discussed in the following section.

CALCULATED ^{239}Pu LLD CONCENTRATIONS

For each of the three spectrum analysis algorithms, the minimum detectable change in net ^{239}Pu counts during each counting interval was calculated using equations presented in Ref. 7, where the calculation was performed at the 95% confidence level. LLD concentrations, expressed as pCi/L, were calculated by inserting the minimum detectable change in net ^{239}Pu counts during each counting interval into the formula for airborne ^{239}Pu concentration given in Ref. 7. In the case of the ANL-W CAM, minimum detectable counts and LLDs were calculated using successive cumulative spectra collected at one hour intervals. Similar results for the Kurz, RADeCO, and Victoreen CAMs were calculated using successive cumulative spectra collected 30 minutes apart. However, spectra collected during selected samplings were also analyzed using successive cumulative spectra collected at 60, 90 and/or 120 minute intervals to determine if increasing the length of the counting interval significantly lowered the ^{239}Pu LLDs.

Calculated ^{239}Pu LLD concentrations, expressed as pCi/L, during a sampling of ambient air performed using the ANL-W CAM are plotted as a function of sampling time in Fig. 8. The concentrations of airborne ^{239}Pu during this sampling determined using the two-, three-, and four-window analysis algorithms are shown in Fig. 1. As previously mentioned, LLDs for the ANL-W CAM were calculated analyzing spectra collected at one hour intervals. Comparing the calculated ^{239}Pu LLDs with the measured ^{239}Pu concentrations for the ANL-W CAM for this sampling of ambient air, it is evident that ^{239}Pu LLD concentrations at the 95% confidence level were well above measured background concentrations of ^{239}Pu during the sampling. Average ^{239}Pu LLDs for the ANL-W CAM during the second

day of sampling were $(2.1 \pm 0.2) \times 10^{-4}$, $(2.2 \pm 0.2) \times 10^{-4}$, and $(1.5 \pm 0.1) \times 10^{-4}$ pCi/L for the two-, three-, and four-window analysis algorithms, respectively. During the fifth day of sampling, LLDs for the corresponding analysis algorithms were $(2.2 \pm 0.2) \times 10^{-4}$, $(2.3 \pm 0.3) \times 10^{-4}$, and $(1.5 \pm 0.1) \times 10^{-4}$ pCi/L, respectively. Thus, the ^{239}Pu LLDs for the two- and three-window algorithms for this sampling of ambient air both averaged about 0.1 DAC while the average ^{239}Pu LLD for the four-window algorithm was slightly lower at about 0.08 DAC using a counting interval of one hour.

Average ^{239}Pu LLDs for the two-, three- and four-window analysis algorithms for the ANL-W CAM for a sampling of ambient air and for the Kurz, RADeCO, and Victoreen CAMs for a sampling of aerosolized spiked dust are summarized in Table II. LLDs for the Kurz, RADeCO, and Victoreen CAMs presented in Table II are average LLDs during the six hours the aerosolizer was operating (i.e., 3½ to 9½ hours), while the results for the ANL-W CAM are average LLDs during the second day of sampling. The data presented in Table II indicate that all four CAMs that were tested have very good sensitivities for ^{239}Pu . When a 30 minute counting interval was used, average LLDs during the sampling of aerosolized spiked dust ranged from

a low of 6.0×10^{-4} pCi/L (0.3 DAC) for the Kurz CAM using the two-window algorithm to a high of 1.45×10^{-2} pCi/L (7.3 DAC) for the Victoreen CAM using the three-window algorithm. When the counting interval was extended to one hour, average LLDs were significantly lower. During the sampling of aerosolized spiked dust, average LLDs determined using a one-hour long counting interval ranged from a low of 2.19×10^{-4} pCi/L (0.1 DAC) for the Kurz CAM using the two-window algorithm to a high of 5.2×10^{-3} pCi/L (2.6 DAC) for the Victoreen CAM using the three-window algorithm. Average LLDs for the ANL-W CAM during the second day of sampling ambient air were about the same for all three algorithms, ranging from low of 1.5×10^{-4} pCi/L (0.08 DAC) using the four-window algorithm to a high of 2.2×10^{-4} pCi/L (0.1 DAC) using the three window algorithm.

As shown in Table II, in the case of the Kurz CAM, the two-window algorithm yielded the lowest average LLD concentration. The average LLD concentration determined using the four-window algorithm was about a factor of three higher while the three-window algorithm was about a factor of 9 higher than the LLD concentration determined using the two-window algorithm. LLD concentrations for the

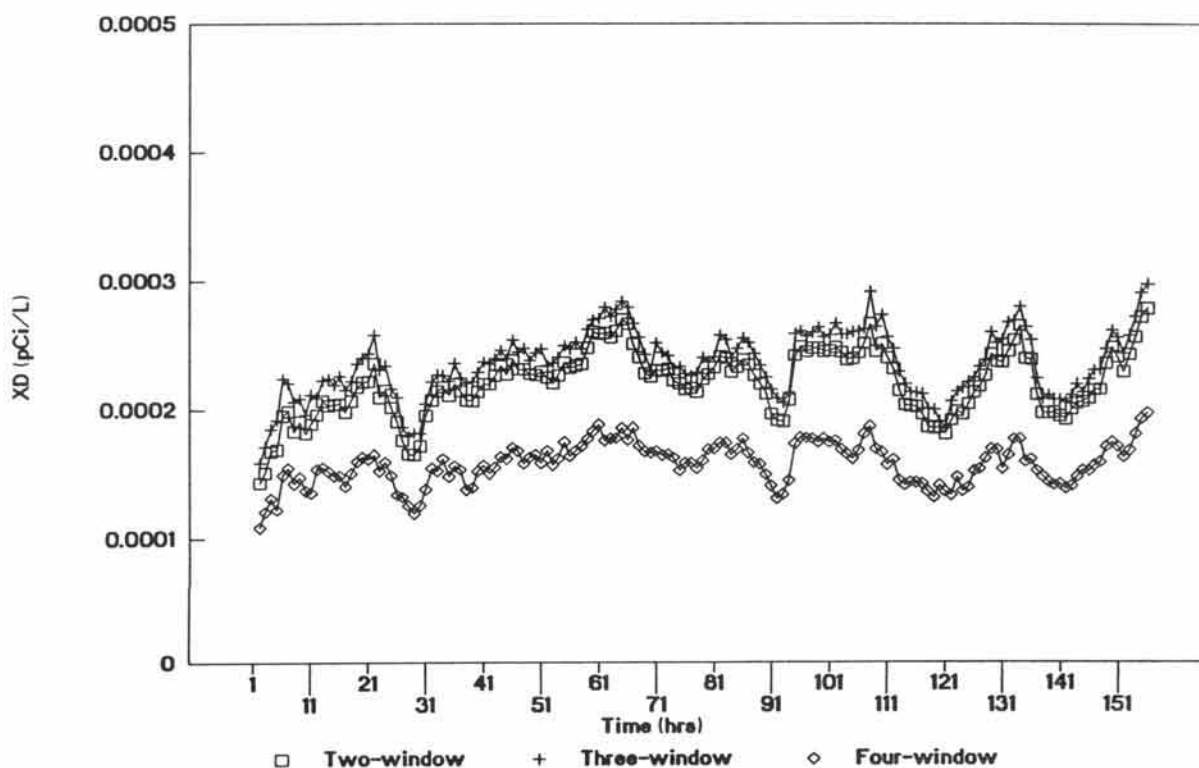


Fig. 8. ^{239}Pu LLD concentration versus sampling time for a sampling of ambient air performed December 20-27, 1989 using the ANL-W CAM.

Kurz CAM for the other five samplings of aerosolized spiked dust showed that this general relationship was universally true for the Kurz CAM. However, during the other samplings, average LLDs for the Kurz CAM that were estimated using the three-window algorithm were generally about a factor of two lower than the results shown in Table II and were in better agreement with the LLDs determined using the two- and four-window algorithms. Average LLDs for the Kurz CAM during the other five samplings of aerosolized spiked dust that were determined using the two- and four-window algorithms were comparable to the corresponding results presented in Table II. Apparently, because the Kurz CAM has such excellent resolution and, therefore, records relatively few background counts in the ^{239}Pu ROI, the simplest background subtraction algorithm worked the best for the Kurz CAM.

In the case of the RADeCO CAM, during the first 60 to 90 minutes after the aerosolizer began operating, LLD concentrations determined using the four-window algorithm were usually higher than LLD concentrations estimated using the two- and three- window algorithms. After this initial period, LLDs calculated for the RADeCO CAM using the four-window algorithm then became about equal to or slightly lower than LLDs determined using the other two algorithms. LLDs determined for three other samplings were comparable to the results for the RADeCO

CAM presented in Table II, while similar results for two other sampling were typically 50% higher.

In the case of the Victoreen CAM, the four-window algorithm consistently yielded the lowest LLD concentrations. The highest LLDs were generally associated with the two-window algorithm, but differences between the high and low LLD concentrations at any given time during any given sampling were typically less than a factor of two. As was the case with the results for the RADeCO CAM, LLDs determined for three other samplings were comparable to the results for the Victoreen CAM presented in Table II, while similar results for two other samplings were typically about 50% higher.

CONCLUSIONS

The measurement results obtained during this study show that the ANL-W, Kurz series 8311, RADeCO model 452, and Victoreen model 758 alpha CAMs each have a lower limit of detection for ^{239}Pu that meets or exceeds the sensitivity requirement of 8 DAC-h that is specified in DOE Order 5480.11. Average ^{239}Pu LLDs for the ANL-W CAM during samplings of ambient air having a dust concentration of about 7×10^{-9} g/L were as low as 0.1 DAC at the 95% confidence level when one-hour long counting intervals were used. Average ^{239}Pu LLDs for the Kurz, RADeCO, and Victoreen CAMs during samplings of air having

TABLE II
Summary of ^{239}Pu LLDs for Selected Samplings

CAM	Average ^{239}Pu LLD Concentration (pCi/L)		
	Two windows	Three windows	Four windows
30 minute counting interval:			
Kurz	$6.0 \pm 0.2 \text{ E}(-04)$	$5.2 \pm 0.2 \text{ E}(-03)$	$1.7 \pm 0.2 \text{ E}(-03)$
RADeCO	$1.01 \pm 0.09 \text{ E}(-02)$	$1.12 \pm 0.04 \text{ E}(-02)$	$8.9 \pm 4.3 \text{ E}(-03)$
Victoreen	$1.2 \pm 0.1 \text{ E}(-02)$	$1.45 \pm 0.06 \text{ E}(-02)$	$7.8 \pm 0.2 \text{ E}(-03)$
60 minute counting interval:			
Kurz	$2.19 \pm 0.05 \text{ E}(-04)$	$1.8 \pm 0.2 \text{ E}(-03)$	$6.1 \pm 0.5 \text{ E}(-04)$
RADeCO	$3.8 \pm 0.4 \text{ E}(-03)$	$1.29 \pm 0.07 \text{ E}(-03)$	$4.1 \pm 2.1 \text{ E}(-03)$
Victoreen	$4.4 \pm 0.4 \text{ E}(-03)$	$5.2 \pm 0.2 \text{ E}(-03)$	$3.0 \pm 0.8 \text{ E}(-03)$
ANL-W	$2.1 \pm 0.2 \text{ E}(-04)$	$2.2 \pm 0.2 \text{ E}(-04)$	$1.5 \pm 0.1 \text{ E}(-04)$

average dust concentrations between about 1×10^{-7} and 5×10^{-7} g/L were, respectively, as low as 0.1, 0.6, and 1.5 DAC at the 95% confidence level when one-hour long counting intervals were used.

The results show that of the analysis algorithms that were tested, the four-window algorithm generally yielded the lowest LLDs for the ANL-W, RADeCO, and Victoreen CAMs and the two-window algorithm consistently produced the lowest LLDs for the Kurz CAM. Detailed information regarding the analysis software that SAIC/RADeCO actually uses in the model 452 CAM was not available when this study was performed and, therefore, their spectrum analysis method was not tested.

The two-stage virtual impactor installed in the ANL-W CAM and the inertial dichotomous impactor installed in the Kurz CAM significantly reduced the number of background counts associated with radon and thoron daughters. The results show that the ANL-W impactor removed, on average, about 97% of the RaA, 95% of the RaC', and 94% of the ThC' from the sample air stream prior to impaction with the sample collection filter. The results also indicate that the Kurz impactor removed, on average, about 37% of the RaA, 88% of the RaC', and 98% of the ThC' from the sample air stream prior to impaction with the surface of the silicon detector. The removal of these indigenous alpha emitters significantly reduced background count rates in the ^{239}Pu ROI. This is reflected in the remarkably low ^{239}Pu LLDs measured for the ANL-W and Kurz CAMs.

However, this benefit must be weighed against the possible detriment associated with discarding some fraction of the particulates initially present in the air being sampled. In the case of the ANL-W CAM, plutonium oxide particles large than $0.4 \mu\text{m}$ geometric diameter are collected on the sample collection filter with greater than 50% efficiency.(4) If in a given measurement environment, fugitive ^{239}Pu aerosols were known to be predominantly greater than $0.4 \mu\text{m}$, then the ANL-W CAM could be used with confidence. If, on the other hand, the size distribution of ^{239}Pu aerosols was unknown or known to include a significant fraction of particles smaller than $0.4 \mu\text{m}$, then the ANL-W CAM

equipped with the existing impactor would probably not be an appropriate CAM to use. The cut point of the Kurz series 8311 impactor has been reported to be about $0.7 \mu\text{m}$ aerodynamic diameter.(6) Results of this study show that, on average, only about 18% of the airborne ^{239}Pu activity that entered the Kurz CAM remained fixed to the surface of the silicon detector following the completion of sampling. It is recommended that the Kurz CAM be subjected to rigorous particle collection efficiency measurements to clarify the activity collection efficiency results obtained in this study.

REFERENCES

1. DOE Order 5480.11, "Radiation Protection for Occupational Workers," U. S. Department of Energy, Washington, D. C. (December 1988).
2. C. V. MCISAAC AND C. R. AMARO, "Real-Time Transuranic Monitoring With a Victoreen Model 758 Alpha Continuous Air Monitor," EGG-WM-8774 (September 1989).
3. G. K. RUSCH, W. P. MCDOWELL, AND W. G. KNAPP, "The ZPR-9 Airborne Plutonium Monitoring System," IEEE Trans. on Nuclear Sci., Vol. NS-23, No. 1 (February 18, 1981).
4. T. J. YULE, "An On-Line Monitor for Alpha-Emitting Aerosols," IEEE Trans. on Nuclear Sci., Vol. NS-23, No. 1 (February 1978).
5. J. M. LARSEN AND D. L. HALL, "ZPPR Plutonium Monitor", ZPR-I Memo No. 389 (February 1976).
6. Model 8311 Alpha Detector User's Guide, 360113, Rev XA2, Preliminary, Kurz Instruments Incorporated (November 1989).
7. "Rapid Monitoring of Transuranics During Buried Waste Retrieval", EG&G-WTD-9412 (January 1991).
8. L. A. CURRIE, "Lower Limit of Detection: Definition and Elaboration of a Proposed Position for Radiological Effluent and Environmental Measurements," NUREG/CR-4007 (September 1984).